The ISME Journal (2014) 8, 504–514

www.nature.com/ismej

ORIGINAL ARTICLE

Dispersal network structure and infection mechanism shape diversity in a coevolutionary bacteria-phage system

Michael Sieber[1], Matthew Robb[2], Samantha E Forde[3] and Ivana Gudelj[1]
[1]*Biosciences, University of Exeter, Exeter, UK;* [2]*Department of Mathematics, Imperial College London, London, UK and* [3]*Ecology and Evolutionary Biology Department, University of California, Santa Cruz, CA, USA*

Resource availability, dispersal and infection genetics all have the potential to fundamentally alter the coevolutionary dynamics of bacteria–bacteriophage interactions. However, it remains unclear how these factors synergise to shape diversity within bacterial populations. We used a combination of laboratory experiments and mathematical modeling to test how the structure of a dispersal network affects host phenotypic diversity in a coevolving bacteria-phage system in communities of differential resource input. Unidirectional dispersal of bacteria and phage from high to low resources consistently increased host diversity compared with a no dispersal regime. Bidirectional dispersal, on the other hand, led to a marked decrease in host diversity. Our mathematical model predicted these opposing outcomes when we incorporated modified gene-for-gene infection genetics. To further test how host diversity depended on the genetic underpinnings of the bacteria-phage interaction, we expanded our mathematical model to include different infection mechanisms. We found that the direction of dispersal had very little impact on bacterial diversity when the bacteria-phage interaction was mediated by matching alleles, gene-for-gene or related infection mechanisms. Our experimental and theoretical results demonstrate that the effects of dispersal on diversity in coevolving host–parasite systems depend on an intricate interplay of the structure of the underlying dispersal network and the specifics of the host–parasite interaction.
The ISME Journal (2014) **8,** 504–514; doi:10.1038/ismej.2013.169; published online 3 October 2013
Subject Category: Microbial population and community ecology
Keywords: coevolution; diversity; dispersal; host–parasite; mathematical model; spatial heterogeneity

Introduction

Microbial diversity is key to many ecosystem processes (Naeem and Li, 1997; Bell *et al.*, 2005; Madsen, 2011), and coevolution among microbes has been suggested as one of the major drivers of biodiversity (Buckling and Rainey, 2002; Forde *et al.*, 2008a). Coevolution is an inherently spatial process that depends not only on the traits of the interacting species but also on the environment in which those interactions take place (Thompson, 1999, 2005; Forde *et al.*, 2004; Parchman and Benkman, 2008; Piculell *et al.*, 2008; Laine, 2009; Craig and Itami, 2010; King *et al.*, 2011; Lorenzi and Thompson, 2011).

There are many ways in which the environment can be spatially structured, but variation in resource input is likely to be one of the major factors influencing coevolutionary dynamics (Hochberg *et al.*, 2000). In particular, experimental studies using bacteria and bacteriophages have demonstrated that the rate of coevolution can increase with increased resources (Forde *et al.*, 2004; Lopez-Pascua and Buckling, 2008), whereas bacterial diversity peaks at intermediate resource levels (Forde *et al.*, 2008a).

High dispersal and the cosmopolitan distribution of bacteria (Brodie *et al.*, 2007; Fahlgren *et al.*, 2010; Yamaguchi *et al.*, 2012) and phages (Breitbart *et al.*, 2004; Angly *et al.*, 2006) across a wide range of environments add additional complexity and the potential to greatly influence microbial diversity (Brockhurst *et al.*, 2007; Vogwill *et al.*, 2008, 2009, 2010). If the abiotic environment does not vary in space, theoretical and experimental studies indicate that dispersal, or gene flow, homogenizes genetic variation (Gandon and Michalakis, 2002; Vogwill *et al.*, 2011). Theory suggests that the same result holds if the abiotic environment varies in space. In particular, Hochberg and van Baalen (1998) predicted that gene flow across spatial gradients in

Correspondence: SE Forde, Ecology and Evolutionary Biology Department, University of California, Santa Cruz, CA 95064, USA. E-mail: forde@biology.ucsc.edu
or I Gudelj, Biosciences, University of Exeter, Exeter EX4 4QD, UK. E-mail: I.Gudelj@exeter.ac.uk
Received 12 July 2013; accepted 17 August 2013; published online 3 October 2013

productivity can lead to a decrease in overall diversity summed across the gradient. However, this theoretical prediction remains experimentally untested.

In the present study, we evaluated how the structure of the dispersal network across a spatial resource gradient affects patterns of bacterial phenotypic diversity in a coevolutionary system consisting of the bacteriophage T3 and its bacterial host *Escherichia coli*. Bacteriophage T3 uses lipopolysaccharides (LPS) as receptors for adsorption to the host cell, and resistance to T3 is conferred through mutations that truncate LPS (Tamaki *et al.*, 1971; Lenski, 1988; Qimron *et al.*, 2006), which can lower bacterial fitness through pleiotropic effects on outer membrane proteins (OMPs) involved in the uptake of resources (Sen and Nikaido, 1991). This bacteria-phage interaction forms the molecular basis for a coevolutionary system conforming to the terminology of the 'Kill the Winner' (KtW) hypothesis (Winter *et al.*, 2010) in the sense that phenotypes with intact LPS structure correspond to competition specialists, whereas truncated LPS structures are a hallmark of a defense specialist.

Our previous work with *E. coli* and phage T3 coevolution in experimental microcosms showed that low resource environments supported more diverse communities than high resource environments (Forde *et al.*, 2008a). Both high and low resource environments contained highly resistant bacterial phenotypes (defense specialists) and highly infective generalist phage. However, whereas these dominated high resource environments leading to low diversity, low resource environments additionally contained sensitive bacterial phenotypes (competition specialists) and their more specialist phage, and as such, were more diverse (Forde *et al.*, 2008a).

Here we considered how the above patterns of bacterial diversity changed when symmetric and asymmetric movement of both bacteria and phage was introduced across the resource gradients. For symmetric (bidirectional) gene flow, we expected the fitness of a given phenotype to be the weighted average of the local fitness it experiences in all habitats along the gradient (Kawecki and Holt, 2002). This should only favor bacteria and phage found in both low- and high-resource habitats, namely defense specialists and highly infective generalist phages (Forde *et al.*, 2008a). This in turn is expected to decrease overall diversity. However, it is less clear *a priori* how unidirectional dispersal should affect bacterial diversity.

In accordance with expectations, we found that bidirectional dispersal decreased diversity compared with when communities were closed. Somewhat surprisingly, however, we found that unidirectional dispersal from high to low resources increased host diversity. Extending the mathematical model in Forde *et al.* (2008a), we showed that these unexpected outcomes are predicted when bacteria-phage interactions follow modified gene-for-gene infection genetics (Forde *et al.*, 2008a).

To further test how the observed dispersal-induced patterns of host diversity depended on the genetic underpinning of the bacteria-phage interactions, we expanded our mathematical model to include different infection mechanisms. This was motivated by the findings in Forde *et al.* (2008a), which showed that the precise nature of the relationship between diversity and resources depended on the infection genetics between bacteria and phages.

Curiously, although in the case of modified gene-for-gene mechanism the different dispersal directions gave rise to different patterns of bacterial diversity, this was not the case for matching alleles (Gandon and Michalakis, 2002; Morgan *et al.*, 2005; Weitz *et al.*, 2005; Forde *et al.*, 2008a), gene-for-gene (Morgan *et al.*, 2005; Forde *et al.*, 2008a; Gandon and Nuismer, 2009) or related infection mechanisms (Nuismer and Otto, 2005; Fenton *et al.*, 2009). These results could be explained by the fact that the modified gene-for-gene mechanism gives rise to 'KtW' dynamics (Winter *et al.*, 2010), whereas the other tested infection mechanisms do not. Our paper illustrates that the effect of dispersal on microbial diversity depends on the intricate interplay of the structure of the dispersal network and precise nature of coevolutionary interactions.

Materials and methods

Experimental design

We coevolved *E. coli* and phage T3 in continuous culture devices known as chemostats (Bohannan and Lenski, 1997) which were connected by dispersal. All chemostats were initially inoculated with isogenic strains of bacteriophage T3 (obtained from the American Type Culture Collection) and *E. coli* (strain REL 607; Bohannan and Lenski, 1997). The volume of each community was maintained at 30 ml, with a washout rate of 0.2 turnovers per h. We directly manipulated resource input and dispersal of T3 and *E. coli* to test how the direction of dispersal along a resource gradient affected local adaptation and diversity. Three levels of resource input were used (high $= 1000\,\mu g\,ml^{-1}$, intermediate $= 100\,\mu g\,ml^{-1}$ or low $= 10\,\mu g\,ml^{-1}$ glucose), whereas the dispersal treatments consisted of unidirectional, bidirectional and no dispersal of the bacteriophages and bacteria together (Figure 1).

Chemostats were sampled every 48 h, concordant with the imposition of the dispersal treatments. For the unidirectional and bidirectional dispersal treatments, ~ 7.5 ml were removed from each chemostat before imposition of the dispersal treatments. Thus, the same volume, containing the entire bacteria-phage community, was removed from each chemostat regardless of the direction of the flow. A portion of each sample was used for the dispersal treatments and to evaluate the phenotypic diversity of the hosts.

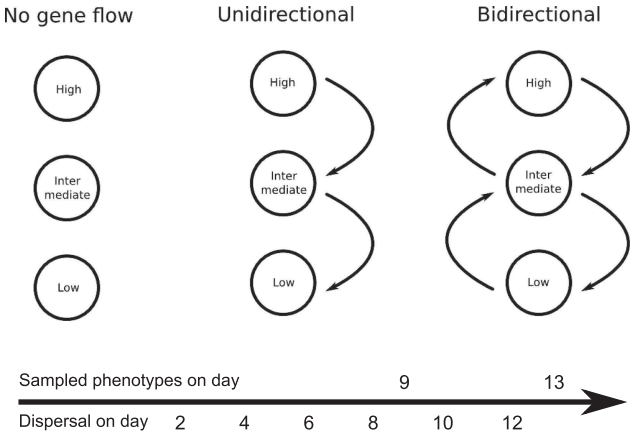

Figure 1 The structure of the dispersal network, labels indicate the different resource levels. Timeline of dispersal and sampling events are shown at the bottom.

In the unidirectional dispersal treatment, 3 ml of the bacteria-phage community were dispersed from the high resource environment to the intermediate environment, and likewise 3 ml from the intermediate to the low resource environment. Three milliliters of sterile saline solution were added to the high resource environment to control for the input volume across treatments (totaling 10% of the total community). In the bidirectional dispersal treatment, 1.5 ml were dispersed from the high into the intermediate environment, and 3 ml from the intermediate into the low resource environment. In the other direction, 1.5 ml were dispersed from the low into the intermediate environment, and 3 ml from the intermediate into the high resource environment. Thus, each community received an input volume totaling 3 ml, regardless of the direction of the flow. Each treatment was replicated three times. The experiment ran for 13 days, or $\sim$200 bacterial generations and 1000 generations of the bacteriophage. During this period, there were seven bouts of dispersal among communities.

Three different reference phage (T2, Tu1a and K3) that attack LPS and different OMPs were used to evaluate phenotypic diversity of the hosts. The three reference phages utilize distinct mechanisms to attack the host, and resistance to them requires different counter-adaptations. For instance, OMPF is the most common OMP of *E. coli* and is involved in osmoregulation and nutrient uptake (Datta *et al.*, 1977; Travisano and Lenski, 1996). Phage T2 uses both OMPF and a part of LPS distal to the T3 receptor to infect *E. coli* cells (Lenski, 1984), so that resistance to T2 indicates that the LPS mutation has also affected the assembly or function of OMPF. Resistance to Tu1a also indicates effects on OMPF (Schwartz, 1980). Resistance to K3 on the other hand indicates that the truncation of LPS has also affected the assembly or function of OMPA (Schwartz, 1980), which is involved in amino-acid transport and the structural integrity of the outer membrane (Morona *et al.*, 1985; Heller, 1992).

Approximately 20 colonies were isolated from the high- and low-resource communities on days 9 and 13 of the experiment each. We did not evaluate host diversity in the intermediate productivity communities. Twenty microliters of each of the three bacteriophages from the screen were then dried on an agar plate and each bacterial isolate was streaked across the bacteriophages to assess whether bacteria were sensitive, partially resistant or completely resistant. Further details on the methodology and cellular biology associated with the phenotypic screen are given in Forde *et al.* (2008b).

This specific screening procedure allowed us to identify up to 27 distinct phenotypes, as for each of the three reference phage exactly three different outcomes of the infection assay were possible. Of those 27 potential phenotypes, a total of 15 were actually observed across all populations (Table 1). The observed frequencies of each phenotype within a population were averaged across replicate chemostats.

Based upon these considerations, phenotypic diversity was calculated using the Shannon-Wiener index in the form

$$H = -\sum_{i=1}^{15} p_i ln(p_i)$$

where p_i is the proportion of phenotype i in the focal host population. Note, that we sum over all 15 observed phenotypes and set $p_i ln(p_i) = 0$ for phenotypes that were not present in the focal community. The results shown throughout the paper are the diversity measures averaged over time. Data were analyzed using analysis of variance with fixed effects (direction of dispersal and resource level) and their interaction.

We also obtained the total number of phenotypes for each dispersal treatment and each resource environment. This measure of phenotype richness and degree of endemicity gives an indication of whether diversity was mediated by phenotypes specific to a resource environment or by phenotypes shared between environments.

In addition, we quantified the resistance of each observed bacterial phenotype against the reference phages (Table 1). For each phenotype, we summed up the level of resistance $r_{n,i}$(0 = sensitive, 0.5 = partially resistant and 1 = resistant) against each of the three reference phages, such that after rescaling the resistance score $R_i = \frac{1}{3}\sum_{n=1}^{3} r_{n,i}$ of a phenotype can range from 0 (universally sensitive) to 1 (universally resistant).

We then calculated the population level of resistance against reference phages in each treatment by multiplying the average local proportions of each phenotype with its resistance score and summing over all phenotypes: $\frac{1}{2}\sum_{i=1}^{15}(p_i^{\mathrm{L}} + p_i^{\mathrm{H}})R_i$, where the superscripts L and H denote proportions in the low and high productivity environments, respectively. This average population resistance

Table 1 Identified phenotypes

Phenotype	*T2*	*Tu1a*	*K3*	*Resistance score*
1	s	s	s	0
2	s	pr	s	0.16
3	s	s	pr	0.16
4	s	r	s	0.33
5	s	s	r	0.33
6	pr	r	s	0.5
7	pr	s	r	0.5
8	s	pr	r	0.5
9	s	r	pr	0.5
10	r	pr	pr	0.66
11	pr	r	pr	0.66
12	s	r	r	0.66
13	r	r	pr	0.83
14	r	pr	r	0.83
15	r	r	r	1

Abbreviations: S, sensitive; pr, partially resistant; r, resistant.

against reference phages is a measure of the probability that a randomly picked cell from either resource environment is resistant against a randomly picked reference phage.

The model

The mathematical model was based on the one developed in Forde *et al.* (2008a) and was designed specifically to capture the biology of microbial coevolution. The deterministic model tracks evolution in initially isogenic populations of co-occurring clonally reproducing bacteria (B_0) and phages (P_0) in the chemostat. Mutations occurred with a small but prescribed probability, and the fitness of mutant bacteria and phages depends on every component of the system (a genotype-by-genotype-by-environment interaction).

T3 phages have higher adsorption rates to wild-type *E. coli* than to contemporary hosts (Chao *et al.*, 1977; Forde *et al.*, 2004; Qimron *et al.*, 2006). Thus, in our initial model, we assumed that the binding probabilities between bacteria and phages are graded (see Sasaki and Godfrey, 1999). As in Forde *et al.* (2008a), we also assumed that there are two character states at two diallelic loci, *L* and *O*, in wild-type bacteria (B_0). We incorporated pleiotropy between LPS and OMPs by assuming that mutations at these loci regulate the biosynthesis of LPS polymers such that the length of the LPS O antigen correlates with the phenotype $T=4-(2\times L+O)$, yielding four phenotypes: $B_0(L=0,O=0)$ with $T=4$; $B_1(0,1)$ with $T=3$; $B_2(1,0)$ with $T=2$; and $B_3(1,1)$ with $T=1$.

We assumed that mutations in the bacteria occurred as point mutations at either *L* or *O* locus with rate ε. Mutations in wild-type phages (P_0) occur at one locus with four possible alleles giving rise to one of three types, denoted P_i (where *i* is from 1 to 3) and the rate of mutations from one phage type to another, ε, is independent of the type of phage. The matrices M_b and M_p modeling mutations between the four bacterial types and the four phage types, respectively, are given in Appendix A.

The core of the *E. coli*–T3 model is a 4×4 matrix that defines the relative infectivities of each phage strain to each bacterial type:

$$\Phi=\sigma\begin{pmatrix}1 & \lambda & \lambda^2 & \lambda^3\\ 0 & \lambda & \lambda^2\nu & \lambda^3\nu\\ 0 & 0 & \lambda^2\nu^2 & \lambda^3\nu^2\\ 0 & 0 & 0 & \lambda^3\nu^3\end{pmatrix} \quad (1)$$

This infection matrix is based on a mechanistic understanding of the attachment process of T3 to its host and as such it is specific to the system under consideration (Forde *et al.*, 2008a). Each column represents one of the four phage types and the respective interactions with the different host strains. For example, the first column corresponds to the wild-type T3 that can only infect wild-type *E. coli*, hence there is a single entry in the first row of this column. Here σ stands for the attachment rate of the wild-type phage, λ represents the change of adsorption rate caused by alterations in the structure of phage tail-fiber protein and ν represents the change in adsorption rate caused by the loss of a single sugar from the bacterial LPS complex with constraints $\lambda<1$, $\nu<2$, respectively. Because of its resemblance to the classical gene-for-gene model (Morgan *et al.*, 2005; Gandon and Nuismer, 2009), this specific model has been termed modified gene-for-gene infection mechanism (Forde *et al.*, 2008a).

In complete analogy to the experimental methods, we can define a resistance score for each bacterial phenotype as the number of phage phenotypes against which it is resistant. This means that the resistance score in the model is simply given by the number of zeros in each row of the infection matrix divided by the total number of phage phenotypes. For the modified gene-for-gene infection mechanism in (1), the resistance score thus ranges from 0 for the wild-type B_0 (competition specialist) to 0.75 for the most, but not completely, resistant type B_3 (defense specialist).

We extended the model in Forde *et al.* (2008a,b) to include dispersal between chemostats of different productivity. Following from the experimental design shown in Figure 1, we considered a scenario in which three chemostats contain different resource levels, resulting from different concentrations of resources in the chemostat input vessels. The rates of change over time in the resource concentration S_i, bacterial densities B_i and phage densities P_i in high-, intermediate- and low resource environments are given by

$$\begin{aligned}\tfrac{dS_i}{dt}&=D\left(S_i^0-S_i\right)-c\mu(S_i)\cdot B_i\\ \tfrac{dB_i}{dt}&=M_b(\mu(S_i)*B_i)-(\Phi P_i)*B_i-DB_i\\ \tfrac{dP_i}{dt}&=M_p\left(\beta*\left(\Phi^T B_i\right)*P_i\right)-DP_i\end{aligned} \quad (2)$$

where the subscript $i = \mathrm{L}$, I, H represents the low, intermediate and high resource environments, respectively. Here, $S_{\mathrm{L}}^0 < S_{\mathrm{I}}^0 < S_{\mathrm{H}}^0$ denote the resource concentrations in the input vessels, whereas B_i and P_i denote the vectors of the four bacterial and phage densities in the different resource environments. The matrix Φ^T is the transposed of the infection matrix. The operators $\cdot$ and * denote the scalar product and component-wise multiplication, respectively.

The first equation of (2) describes the rate of change in resource concentration in the three chemostats, where the constant D represents the chemostat washout rate. Resource consumption is modeled using a Michaelis–Menten bacterial growth vector function μ and resource conversion rate c. The phage production is represented by a vector of burst sizes β; however, latent period was not explicitly modeled. Bacterial costs for resistance are mediated by phenotype-specific maximal growth rates, which are incorporated into the growth vector function μ. Similarily, an increase in phage host range is traded-off with a decrease in burst size, described by the burst size vector β (Ferris *et al.*, 2007; Poullain *et al.*, 2008). For a further description of the model in the absence of spatial structure see Appendix A.

Unidirectional and bidirectional dispersal between high ($i = \mathrm{H}$), intermediate ($i = \mathrm{I}$) and low resource ($i = \mathrm{L}$) environments was incorporated into the model in the following way. After a simulated time of N hours, the simulation was stopped and the densities of resources, bacteria and phages in the three chemostats were reduced by 25%, representing the removal of 7.5 ml of the total chemostat volume of 30 ml. Then the dispersal treatment was imposed by increasing the densities in the receiving chemostats by the appropriate amount, which depends on the predispersal densities in the source chemostat and the dispersal treatment. For example, in the unidirectional treatment, the low productivity chemostat received a sample of 10% of the whole resource-bacteria-phage community of the intermediate productivity chemostat, corresponding to 3 ml of volume. After this procedure, the simulation of system (2) was started again and run until the next dispersal event. In this way, complete analogy with the experiments was maintained. All parameters in model (2) are from Forde *et al.* (2008a) and are shown in Table 2.

To test how the model results depend on the form of host–parasite interactions, we also included matching alleles, gene-for-gene, inverse matching alleles and inverse gene-for-gene infection genetics in our analysis. The detailed forms of these infection matrices can be found in Appendix A.

Results

Experiment

The results of the phenotypic diversity assay are displayed in Figure 2a. Diversity differed markedly among the dispersal treatments and an analysis of variance showed that the direction of dispersal had a significant effect on diversity, whereas there was no effect of resource level or interaction between factors (Table 3). Unidirectional dispersal increased diversity compared with no dispersal (P-value = 0.045), in particular in the high resource environment. Bidirectional dispersal on the other hand had an overall negative effect on diversity compared with no dispersal (P-value = 0.01) and unidirectional dispersal (P-value < 0.0001).

For the no dispersal and bidirectional treatments, an equal total number of phenotypes were identified, whereas the highest total number of phenotypes was observed in the unidirectional treatment (Figure 3). The fraction of locally specific types was highest for the no dispersal treatment and lower in the unidirectional and bidirectional treatments (Figure 3b).

The global proportions of identified phenotypes within each dispersal treatment were obtained as the average frequency of each type across resource environments (Figure 3a). In contrast to the no dispersal and unidirectional flow treatments, the meta-population in the bidirectional treatment is dominated by just two phenotypes, which explains the lower level of diversity in this treatment.

The average level of resistance against reference phage for each treatment, along with the relative contribution of each phenotype to the population

Table 2 Parameter values for model (2)

Parameter	*Description*	*Value*
μ_i^{max}	Maximal growth rate of bacterial type i	$\mu_0^{max} = 1.18\,\mathrm{h}^{-1}$, $\mu_1^{max} = 1.009\,\mathrm{h}^{-1}$, $\mu_2^{max} = 0.89\,\mathrm{h}^{-1}$, $\mu_3^{max} = 0.66\,\mathrm{h}^{-1}$
K	Bacterial half saturation constant	$0.06\,\mu\mathrm{g\,ml}^{-1}$
β_i	Burst size of phage i	$\beta_0 = 306$, $\beta_1 = 153$, $\beta_2 = 99$, $\beta_3 = 72$ virions per cell
D	Chemostat dilution rate	$0.2\,\mathrm{h}^{-1}$
ε	Rate of point mutations	10^{-4}
c	Resource conversion rate	$2.3 \times 10^{-5}\,\mu\mathrm{g}$ per cell
S_i^0	Resource in parameter	$S_H^0 = 10^3\,\mu\mathrm{g\,ml}^{-1}$, $S_I^0 = 10^2\,\mu\mathrm{g\,ml}^{-1}$, $S_L^0 = 10\,\mu\mathrm{g\,ml}^{-1}$
σ	Wild-type T3 attachment rate	$2 \times 10^{-8}\,\mathrm{ml\,h}^{-1}$
ν,λ	Infectivity parameters fitted in Forde *et al.* (2008a,b)	$\nu = 0.677$, $\lambda = 0.94$

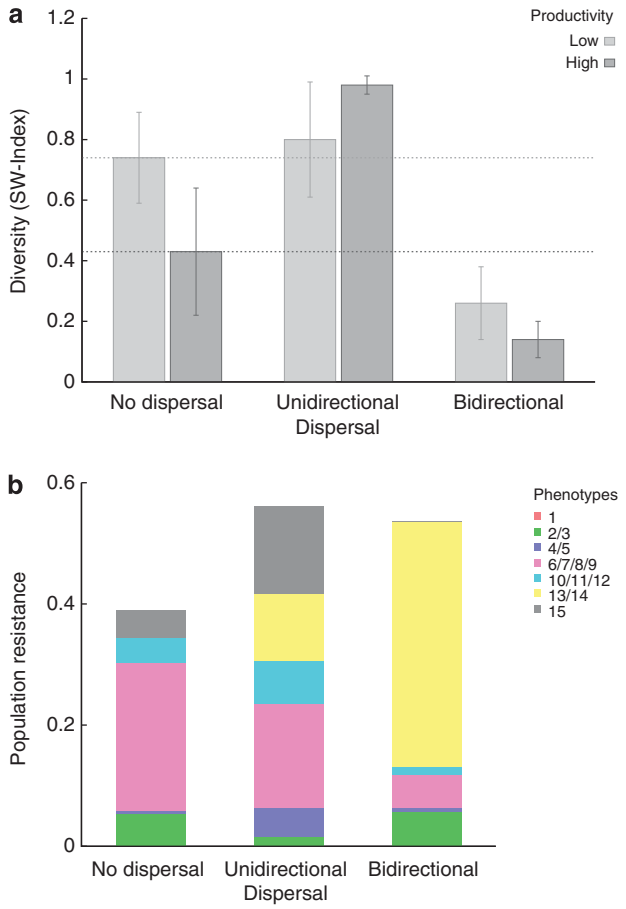

Figure 2 (**a**) Host diversity (Shannon-Wiener index ± s.e.m.) in the high (dark grey) and low (light grey) resource environments for the three different dispersal treatments. Dotted lines were used to guide the eye highlighting host diversity levels in high (dark grey dots) and low (light grey dots) resource environments in the absence of dispersal. (**b**) Population resistance against reference phages as a proxy for bacterial resistance against the wild-type T3 phage. Bar length gives the average population resistance for each dispersal treatment. Phenotypes have been grouped according to their average resistance against the reference phage, and the partitioning of each bar indicates the contribution of each group to the mean population resistance.

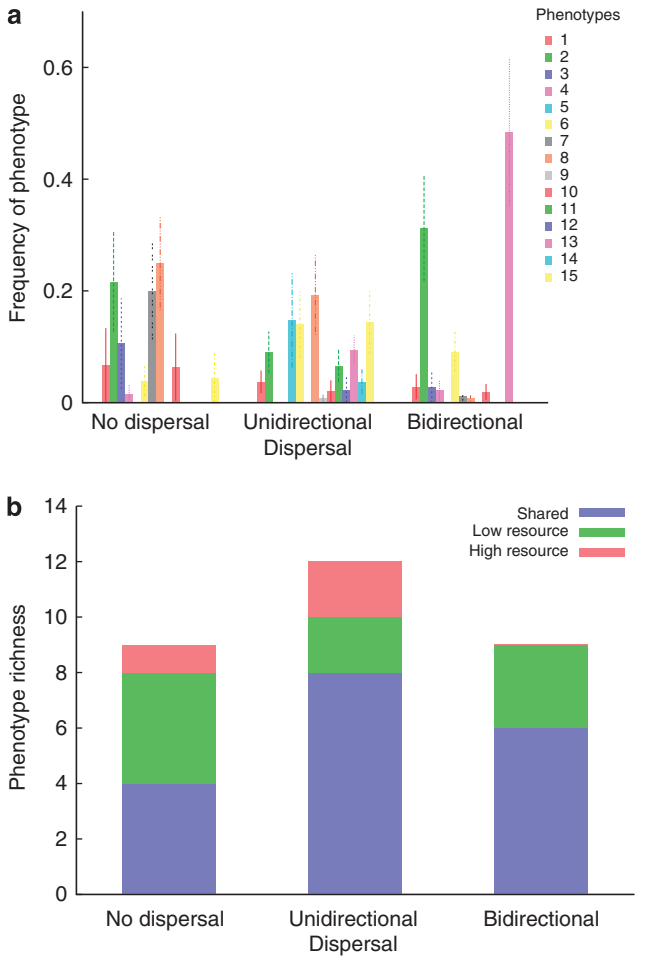

Figure 3 (**a**) Proportions of identified host phenotypes (Table 1) for the three different dispersal treatments across both resource environments. For each dispersal treatment, the phenotypes are placed on the *x* axis in order of ascending resistance against the reference phages, from the universally sensitive type 1 on the left to the universally resistant type 15 on the right (see text for details). (**b**) Phenotype richness and endemicity. Each bar indicates the total number of identified phenotypes for each of the three dispersal treatments, partitioned into the number of phenotypes that were present in both resource environments (blue); only in the low resource environments (green); only in the high resource environments (red).

Table 3 Analysis of variance for experimental results of host diversity

Source	*Sum square*	*d.f.*	*Mean square*	F	*Probability*>F
Gene flow direction	2.17816	2	1.08908	17.89	<0.0001
Resource	0.03859	1	0.03859	0.63	0.4363
Gene flow × resource	0.18694	2	0.09347	1.54	0.2423
Error	1.09592	18	0.06088		
Total	3.65280				

Abbreviation: d.f., degree of freedom.

level resistance against reference phage, is shown in Figure 2b. This serves as a proxy for assessing the resistance to the wild-type T3 phage. For example, resistance to the reference phages signifies changes in LPS, OMPF and/or OMPA which can be used to infer whether a given phenotype has mostly intact LPS structure (low resistance score) or truncated LPS (high resistance score) required for the resistance to T3 (Tamaki *et al.*, 1971; Lenski, 1988; Qimron *et al.*, 2006). Although the average level of resistance is similar in all three dispersal treatments, the contribution of different phenotypes is consistent with the differing levels of diversity (Figure 2b). In the no dispersal and unidirectional treatments, the population level resistance is mediated by several different types with varying degrees of resistance, whereas the level of resistance in the bidirectional treatment can mainly be attributed to one single highly resistant phenotype.

Model

Using deterministic simulations of model (2), we calculated diversity for each directional treatment (see Materials and methods for details) and to maintain consistency with the experiments, diversity was averaged over time.

In order to relate theoretical predictions to experimental data of *E. coli*–T3 interactions, we first considered the modified gene-for-gene mechanism (1). In the absence of dispersal, the model predicted greater host diversity in low resource environments compared with high resource environments (Figure 4a), which was in agreement with the experimental results (Figure 2a).

We fine-tuned the dispersal rate in the model by using the experimentally observed patterns of phenotypic diversity (Figure 2a). Model predictions (Figure 4a) aligned with the experimental results (Figure 2a) for dispersal rates higher than those used in the experiment. This discrepancy could be due to the relative simplicity of the model that combines bacterial diversity into four phenotypes. This naturally also led to consistently lower absolute levels of diversity (Figure 4a) than observed experimentally (Figure 2a). However, it is the simplicity of the model that enabled us to interpret experimental findings in a broader context as explained in the Discussion.

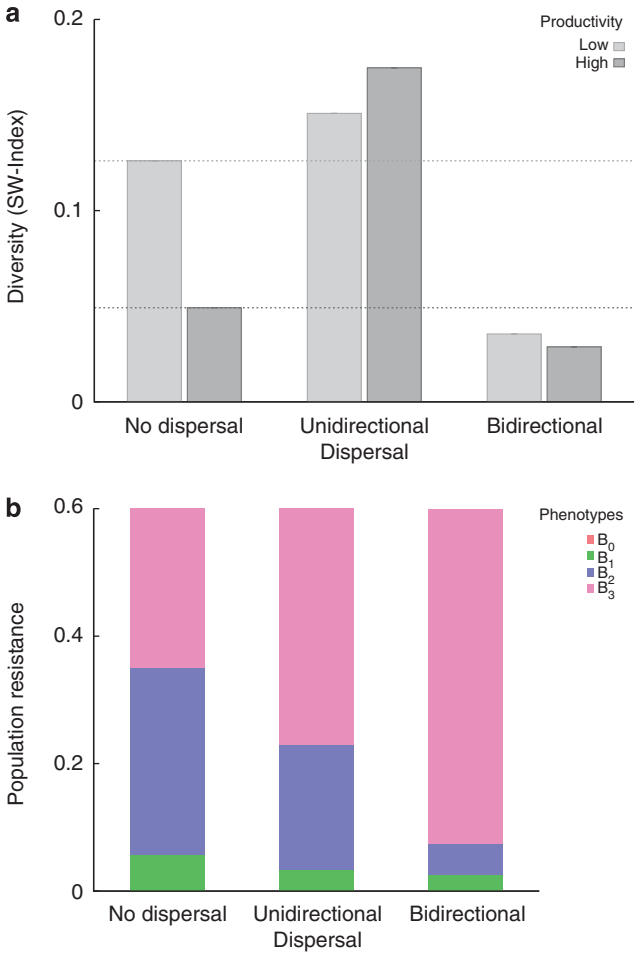

Figure 4 (**a**) Bacterial diversity as predicted by model (2) with modified gene-for-gene infection mechanism in high (dark grey) and low (light grey) resource environments. Dotted lines highlight host diversity levels in high (dark grey) and low (light grey) resource environments in the absence of dispersal. Dispersal rate was set to 6 h. (**b**) Average population resistance against the wild-type T3 phage as predicted by model (2) with modified gene-for-gene infection mechanism. Each color represents one of the four phenotypes from the theoretical model.

Turning to the population level of resistance, the model predicted that resistance against wild-type T3 under the bidirectional treatment is conferred almost exclusively through the dominance of the most resistant type (Figure 4b). This is in agreement with experimental results in Figure 2b, which depict bacterial resistance against reference phages and supports our use of population resistance against reference phage as a proxy for bacterial resistance against the wild-type T3. Under the other two modes of dispersal, the model predicted that a significant proportion of a less resistant type was maintained in the population, which is broadly in agreement with the experimental results (Figure 2b). The model does not capture the precise population composition observed in the experiments due to its simplification of grouping bacterial diversity into four phenotypes.

Model predictions did not change when we removed the intermediate resource environment from our model and instead only considered low and high resource environments linked by dispersal. This could be explained by the observation that in the absence of dispersal, the intermediate resource environment followed the pattern of diversity observed in the high resource environment (Supplementary Figure B1, Appendix B).

We next tested our hypothesis that the effect of dispersal across productivity gradients on host diversity depends not only on the structure of the dispersal network but also on the infection genetics of bacteria and phages. Therefore, we replaced the modified gene-for-gene interaction matrix (1) with the matching alleles, gene-for-gene, inverse matching alleles and inverse gene-for-gene models described in the Appendix B.

In line with previous results, in the absence of dispersal, the model with matching alleles infection mechanism predicted coexistence of all four bacterial types at similar densities in both resource environments (Forde *et al.*, 2008a). As a consequence, we observed markedly higher levels of diversity independent of habitat productivity (Figure 5a). Moreover, neither unidirectional nor bidirectional dispersal had a visible impact on bacterial community composition and the observed levels of diversity (Figure 5a).

The results with the classical gene-for-gene infection mechanism were very similar to the matching alleles model. Bacterial populations were dominated mainly by equal proportions of the two host

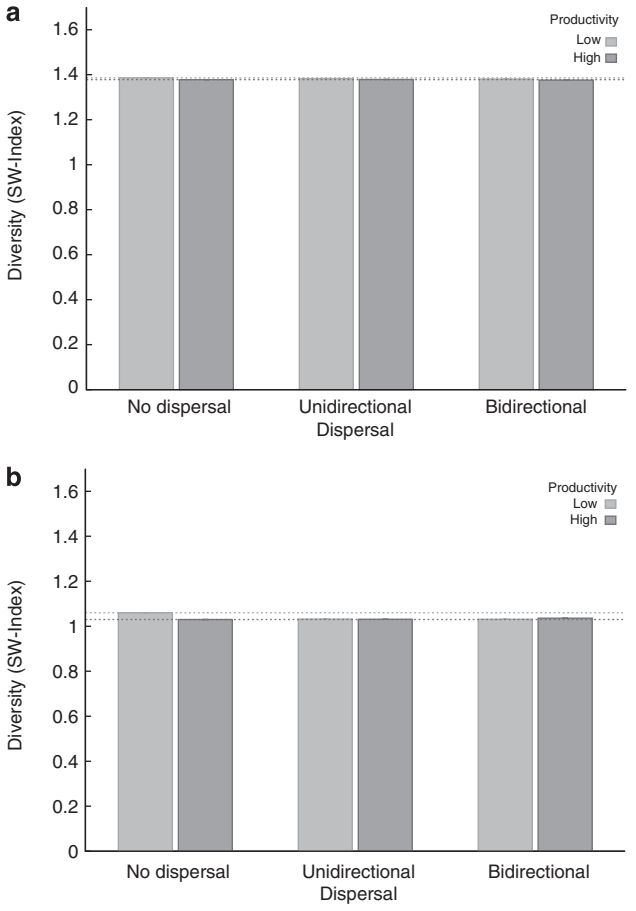

Figure 5 Bacterial diversity in high (dark grey) and low (light grey) resource environments as predicted by model (2) with matching alleles infection mechanism (**a**) and gene-for-gene infection mechanism (**b**). Dotted lines highlight host diversity levels in high (dark grey dots) and low (light grey dots) resource environments in the absence of dispersal.

types with intermediate resistance, such that diversity was higher overall and there was no difference between resource environments (Figure 5b). In addition, diversity did not change in response to different dispersal modes (Figure 5b). Note, that similar marginal effects on diversity were also obtained with inverse matching alleles and inverse gene-for-gene infection genetics.

Discussion

We combined experimental coevolution of bacteria and phages with mathematical modeling to determine the effects of dispersal across a productivity gradient on bacterial diversity. We found that dispersal of bacteria and phages had a marked effect on overall host diversity compared with diversity in the absence of dispersal, but patterns of diversity depended on the structure of the dispersal network. When communities were connected by bidirectional dispersal, bacterial diversity decreased in all habitats across the productivity gradient (Figure 2), as expected from previous results (Hochberg and van Baalen, 1998; Vogwill *et al*., 2011). Unexpectedly, unidirectional dispersal from high to low productivity habitats increased bacterial diversity in the source habitat and had only a small effect on the downstream community (Figure 2), leading to an overall increase in diversity.

This differential effect of the two dispersal networks can be understood within the framework of the 'KtW' hypothesis (Winter *et al*., 2010). KtW assumes that bacterial phenotypes employ evolutionary strategies ranging from competition specialists (efficiently growing, but phage-sensitive) to defense specialists (slower growing, but phage-resistant). The modified gene-for-gene infection mechanism mediating the interaction between *E. coli* and T3 (Forde *et al*., 2008a) conforms to the assumptions of KtW. Here wild-type bacteria with intact LPS structures correspond to competition specialists, whereas phenotypes with one or several LPS truncations are at the defense specialist end of the strategy spectrum, as truncations in LPS can have pleiotropic effects on OMPs involved in the uptake of nutrients (Sen and Nikaido, 1991).

In accordance with central predictions of KtW and previous results (Bohannan and Lenski, 2000; Forde *et al*., 2008a), we found that without dispersal, low resource environments allowed the coexistence of competition specialists and a smaller fraction of defense specialists, whereas in high resource environments, costly mutations conferring resistance against phages were effectively mitigated by abundant resources and thus allowed defense specialists to dominate (Forde *et al*., 2008a). As a consequence, low resource environments were more phenotypically diverse compared with high resource environments (Figure 2).

When bacteria and phages were dispersed together bidirectionally across the resource gradient, the defense specialists, which were able to persist under both environmental conditions, became the dominant phenotype in all habitats. Thus, as expected from theoretically predictions (Hochberg and van Baalen, 1998; Kawecki and Holt, 2002), overall diversity decreased when dispersal was bidirectional (or symmetrical) across the heterogeneous landscape.

In contrast to the prediction by Hochberg and van Baalen (1998) that dispersal across a resource gradient should decrease diversity, we found that unidirectional dispersal from high to low resource environments increased overall diversity. A possible explanation for our result is that although the high productivity community did not receive any input of non-endemic phenotypes, the repeated loss of a fraction of the microbial population during dispersal events may have opened up a niche for the competition specialists. Our theoretical model suggests that the decrease in density of defense specialists and the associated lower rates of phage predation after a dispersal event can allow a small

subpopulation of competition specialists to temporarily reach high population densities. If dispersal is not too infrequent, this transient effect is enough to allow the competition specialists to persist in the high productivity environment. Thus, a decrease in density-dependent competition as a side-effect of the dispersal process itself led to the observed increase in diversity in the upstream high resource environment, rather than any actual dispersal-mediated gene flow.

Our theoretical study of different infection mechanisms further suggests that the presence of different phenotypic strategies in different environments is in fact necessary for dispersal to have a marked effect on diversity. The matching-alleles infection mechanism, for example, led to a higher overall bacterial diversity, but in this case the different phenotypes all represent the same evolutionary strategy with equal competitive abilities and resistance against phages. Thus, all phenotypes coexist in similar proportions in all environments across the productivity gradient and dispersal between habitats can have no effect on local phenotypic diversity.

A similar rationale applies to the gene-for-gene and related infection mechanisms, such as inverse matching alleles and inverse gene-for-gene. Whenever the infection mechanism mediating the bacteria-phage interaction does not promote the emergence of a locally specific set of phenotypic strategies, in the sense of the KtW hypothesis, the effect of dispersal on local diversity can only be marginal.

The form of dispersal we considered in our study is typical for, but not limited to, aquatic habitats, where bacteria and phages are passively transported together with the surrounding aquatic environment. The effect of riverine network structure on biodiversity is of great importance in freshwater ecology (Nelson *et al*., 2009; Brown *et al*., 2011), but its effects on microbial diversity are under-researched. Our results shed light on how local selection for distinct phenotypic strategies and dispersal work together to shape microbial diversity in aquatic networks. We further illustrate that dispersal events can pose significant perturbations of upstream communities, which allow the local rare biosphere (Sogin *et al*., 2006) to fill newly opened niches and flourish temporarily. This is a usually overlooked aspect of dispersal with the potential to alter the course of coevolution and induce a permanent shift in microbial community composition.

Our theoretical model further predicts that dispersal rates have an effect on bacterial community composition (Supplementary Figure B2, Appendix B), in line with dispersal experiments involving freshwater bacteria in their natural lake water environments (Lindström and Östman, 2011). Our model also suggests that unidirectional dispersal tends to increase overall bacterial diversity, regardless of the strength of the transport flow (Supplementary Figure B2a, Appendix B). Interestingly, the relationship between dispersal strength and diversity is more complex in bidirectional networks, suggesting that high dispersal rates have a negative impact on overall diversity, whereas low to moderate dispersal rates tend to increase diversity (Supplementary Figure B2b, Appendix B). These theoretical results have implications for the potential impact of altered flow regimes (Bunn and Arthington, 2002) on microbial community composition.

In summary, our combination of *in vitro* experiments and mathematical models suggests that the effect of dispersal on microbial diversity depends on an intricate interplay of the abiotic characteristics of habitats within a dispersal network and the specific mechanism mediating the interaction of the coevolutionary players. If the heterogeneous landscape supports the formation of locally distinct ecological strategies following a KtW pattern, bidirectional dispersal tends to favor defense specialist strategies and thus decreases diversity. Unidirectional dispersal, on the other hand, can increase diversity in high productivity upstream communities by disturbing the resident defense specialists, thereby opening up niches for competition specialists. These findings could be taken further and used to shed light on why are certain marine bacteria so successful (Zhao *et al*., 2013).

Acknowledgements

We thank JN Thompson for editorial comments on the manuscript. IG was supported by a NERC Advanced Fellowship, SEF was funded by the National Science Foundation DEB 0515598 and MR was supported by a NERC PhD studentship. IG, SEF and MS were also funded by a BBSRC/NSF EEID grant.

References

Angly FE, Felts B, Breitbart M, Salamon P, Edwards RA, Carlson C *et al*. (2006). The marine viromes of four oceanic regions. *PLoS Biol* **4**: 2121–2131.

Bell T, Newman JA, Silverman BW, Turner SL, Lilley AK. (2005). The contribution of species richness and composition to bacterial services. *Nature* **436**: 1157–1160.

Bohannan BJM, Lenski RE. (1997). The effect of resource enrichment on a chemostat community of bacteria and phage. *Ecology* **78**: 2303–2315.

Bohannan BJM, Lenski RE. (2000). The relative importance of competition and predation varies with productivity in a model community. *Am Nat* **156**: 329–340.

Breitbart M, Miyake JH, Rohwer F. (2004). Global distribution of nearly identical phage-encoded DNA sequences. *FEMS Microbiol Lett* **236**: 249–256.

Brockhurst MA, Buckling A, Poullain V, Hochberg ME. (2007). The impact of migration from parasite-free patches on antagonistic host-parasite coevolution. *Evolution* **61**: 1238–1243.

Brodie EL, DeSantis TZ, Moberg Parker JP, Zubietta IX, Piceno YM, Anderson GL. (2007). Urban aerosols harbor diverse and dynamic bacterial populations. *PNAS* **104**: 299–304.

Brown BL, Swan CM, Auerbach DA, Campbell Grant EH, Hitt NP, Maloney KO *et al.* (2011). Metacommunity theory as a multispecies, multiscale framework for studying the influence of river network structure on riverine communities and ecosystems. *J N Am Benthol Soc* **30**: 310–327.

Buckling A, Rainey PB. (2002). Antagonistic coevolution between a bacterium and bacteriophage. *Proc R Soc B* **269**: 931–936.

Bunn SE, Arthington AH. (2002). Basic principles and ecological consequences of altered flow regimes for aquatic biodiversity. *Environ Manage* **30**: 492–507.

Chao L, Levin BR, Stewart FM. (1977). A complex community in a simple habitat: an experimental study with bacteria and phage. *Ecology* **58**: 369–378.

Craig TP, Itami KJ. (2010). Divergence of *Eurosta solidagninis* in response to host plant variation and natural enemies. *Evolution* **65**: 802–817.

Datta DB, Arden B, Henning U. (1977). Major proteins of the *Escherichia coli* outer cell envelope membrane as bacteriophage receptors. *J Bacteriol* **131**: 821–829.

Fahlgren C, Hagström A, Nilsson D, Zweifel UL. (2010). Annual variations in the diversity, viability, and origin of airborne bacteria. *Appl Environ Microbiol* **76**: 3015–3025.

Fenton A, Antonovics J, Brockhurst MA. (2009). Inverse-gene-for-gene infection genetics and coevolutionary dynamics. *Am Nat* **174**: 230–242.

Ferris MT, Joyce P, Burch CL. (2007). High frequency of mutations that expand the host range of an RNA virus. *Genetics* **176**: 1013–1022.

Forde SE, Thompson JN, Bohannan BJM. (2004). Adaptation varies through space and time in a coevolving host-parasitoid interaction. *Nature* **431**: 841–844.

Forde SE, Beardmore RE, Gudelj I, Arkin S, Thompson JN, Hurst LD. (2008a). Understanding the limits to generalizability of experimental evolutionary models. *Nature* **455**: 220–224.

Forde SE, Thompson JN, Bohannan BJM, Holt RD. (2008b). Coevolution drives temporal changes in fitness and diversity across environments in a bacteria-bacteriophage interaction. *Evolution* **62**: 1830–1839.

Gandon S, Nuismer SL. (2009). Interactions between genetic drift, gene flow and selection mosaics drive parasite local adaptation. *Am Nat* **173**: 212–224.

Gandon S, Michalakis Y. (2002). Local adaptation, evolutionary potential and host–parasite coevolution: interactions between migration, mutation, population size and generation time. *J Evol Biol* **15**: 451–462.

Heller KJ. (1992). Molecular interaction between bacteriophage and the gram negative cell envelope. *Arch Microbiol* **15**: 235–248.

Hochberg ME, van Baalen M. (1998). Antagonistic coevolution over productivity gradients. *Am Nat* **152**: 620–634.

Hochberg ME, Gomulkiewicz R, Holt RD, Thompson JN. (2000). Weak sinks could cradle mutualisms - strong sources should harbor pathogens. *J Evol Biol* **13**: 213–222.

Kawecki TJ, Holt RD. (2002). Evolutionary consequences of asymmetric dispersal rates. *Am Nat* **160**: 333–347.

King K, Delph LF, Jokela J, Lively CM. (2011). Coevolutionary hotspots and coldspots for host sex and parasite local adaptation in a snail-trematode interaction. *Oikos* **120**: 1335–1340.

Laine AL. (2009). Role of coevolution in generating biological diversity: spatially divergent selection trajectories. *J Exp Bot* **60**: 2957–2970.

Lenski RE. (1988). Experimental studies of pleiotropy and epistasis in *Escherichia coli* I. Variation in competitive fitness among mutants resistant to virus T4. *Evolution* **42**: 425–432.

Lenski RE. (1984). Two-step resistance by *Escherichia coli* B to bacteriophage T2. *Genetics* **107**: 1–7.

Lindström ES, Östman Ö. (2011). The importance of dispersal for bacterial community composition and functioning. *PloS One* **6**: e25883.

Lopez-Pascua LDC, Buckling A. (2008). Increasing productivity accelerates host–parasite coevolution. *J Evol Biol* **21**: 853–860.

Lorenzi MC, Thompson JN. (2011). The geographic structure of selection on a coevolving interaction between social parasitic wasps and their hosts hampers social evolution. *Evolution* **65**: 3527–3542.

Madsen EL. (2011). Microorganisms and their roles in fundamental biogeochemical cycles. *Curr Opin Biotechnol* **22**: 456–464.

Morgan AD, Gandon S, Buckling A. (2005). The effect of migration on local adaptation in a coevolving host-parasite system. *Nature* **437**: 253–256.

Morona R, Krämer C, Henning U. (1985). Bacteriophage receptor area of outer membrane protein OmpA of *Escherichia coli*. *J Bacteriol* **164**: 539–543.

Naeem S, Li S. (1997). Biodiversity enhances ecosystem reliability. *Nature* **390**: 507–509.

Nelson CE, Sadro S, Melack JM. (2009). Constrasting influences of stream inputs and landscape position on bacterioplankton community structure and dissolved organic composition in high-elevation lake chains. *Limnol Oceanogr* **54**: 1292–1305.

Nuismer SL, Otto SP. (2005). Host-parasite interactions and the evolution of gene expression. *PloS Biol* **3**: e203.

Parchman TL, Benkman CW. (2008). The geographic selection mosaic for ponderosa pine and crossbills: a tale of two squirrels. *Evolution* **62**: 348–360.

Piculell BJ, Hoeksema JD, Thompson JN. (2008). Interactions of biotic and abiotic environmental factors on an ectomycorrhizal symbiosis, and the potential for selection mosaics. *BMC Biol* **6**: 23.

Poullain V, Gandon S, Brockhurst MA, Buckling A, Hochberg ME. (2008). The evolution of specificity in evolving and coevolving antagonistic interactions between a bacteria and its phage. *Evolution* **62**: 1–11.

Qimron U, Marintcheva B, Tabor S, Richardson CC. (2006). Genomewide screens for *Escherichia coli* genes affecting growth of T7 bacteriophage. *PNAS* **103**: 19039–19044.

Sasaki A, Godfray HCJ. (1999). A model for the coevolution of resistance and virulence in coupled host-parasitoid interactions. *Proc R Soc B* **266**: 455–463.

Schwartz M. (1980). Interaction of phages with their receptor proteins. In: Randall LL, Philipson L (eds *Virus Receptors, Part 1 Bacterial Viruses*. Chapman Hall: New York, NY, USA, pp 59–94.

Sen K, Nikaido H. (1991). Lipopolysaccharide structure required for *in vitro* trimerization of *Escherichia coli* OmpF porin. *J Bacteriol* **173**: 926–928.

Sogin ML, Morrison HG, Huber JA, Welch DM, Huse SM, Neal PR *et al.* (2006). Microbial diversity in the deep sea and the underexplored 'rare biosphere'. *PNAS* **103**: 12115–12120.

Tamaki S, Tomoyasu S, Matsuhashi M. (1971). Role of lipopolysaccharides in antibiotic resistance and bacteriophage adsorption of *Escherichia coli* K-12. *J Bacteriol* **105**: 968–975.

Thompson JN. (1999). Specific hypotheses on the geographic mosaic of coevolution. *Am Nat* **153**: S1–S14.

Thompson JN. (2005). *The Geographic Mosaic Theory of Coevolution*. Chicago Univ Press: Chicago, IL, USA.

Travisano M, Lenski RE. (1996). Long-term experimental evolution in *Escherichia coli*. IV. Targets of selection and the specificity of adaptation. *Genetics* **143**: 15–26.

Vogwill T, Fenton A, Brockhurst MA. (2008). The impact of parasite dispersal on antagonistic host-parasite coevolution. *J Evol Biol* **21**: 1252–1258.

Vogwill T, Fenton A, Buckling A, Hochberg ME, Brockhurst MA. (2009). Source populations act as coevolutionary pacemakers in experimental selection mosaics containing hotspots and coldspots. *Am Nat* **173**: 171–176.

Vogwill T, Fenton A, Brockhurst MA. (2010). How does spatial dispersal network affect the evolution of parasite local adaptation? *Evolution* **64**: 1795–1801.

Vogwill T, Fenton A, Brockhurst MA. (2011). Coevolving parasites enhance the diversity-decreasing effect of dispersal. *Biol Lett* **7**: 578–580.

Weitz JS, Hartman H, Levin SA. (2005). Coevolutionary arms races between bacteria and bacteriophage. *PNAS* **102**: 9535–9540.

Winter C, Bouvier T, Weinbauer MG, Thingstad TF. (2010). Trade-offs between competition and defense specialists among unicellular planktonic organisms: the ''Killing the Winner'' hypothesis revisited. *Microbiol Mol Biol Rev* **74**: 42–57.

Yamaguchi N, Ichijo T, Sakotani A, Baba T, Nasua M. (2012). Global dispersion of bacterial cells on Asian dust. *Sci Rep* **2**: 525.

Zhao Y, Temperton B, Thrash JC, Schwalbach MS, Vergin KL, Landry ZC *et al.* (2013). Abundant SAR11 viruses in the ocean. *Nature* **494**: 357–360.

Supplementary Information accompanies this paper on The ISME Journal website (http://www.nature.com/ismej)

Supplementary Material

Appendix A: Formulation of a spatially unstructured model

Growth

For a given resource environment, the mathematical model presented in this paper was developed in (Forde et al 2008). Below we revisit the main assumptions while the detailed explanation and analysis of this model can be found in Supplementary Information of Forde et al 2008.

Let B_i and P_i (where i = 0, ...,3) denote the densities of bacterial and phage types, respectively. Each bacterial type B_i metabolises glucose, of concentration S, in the environment at time t. The growth rate of that type is given by a Monod term:

$$\mu_i(S) = \frac{\mu_i^{\max} S}{K + S},$$

where $\mu_i^{\max}$ denotes the maximal growth rate and K the affinity for resource of the bacteria. All bacterial types are assumed to have the same affinity for resource, but they differ in their maximal growth rates with $\mu_0^{\max} > \mu_1^{\max} > \mu_2^{\max} > \mu_3^{\max}$.

Infection

In order to represent virion-bacterium adsorption we assumed a mass-action law to be valid, as is known to hold up to some concentration (see Gamow, 1969 for T4 phage where this is stated to hold up to a concentration of 2×10^8 bacteria per milliliter). We also assumed that different phage types with different host ranges have different burst sizes (Ferris et al., 2007) and that when a phage of type i infects a bacterium, it replicates by means of the lytic life cy-

cle causing lysis of the host in order to release β_i new free virions, although the latent period was not included in the model.

The rates of adsorption of each virion of type *i* to each bacterium of type *j* are stored within a 4×4-square infection matrix Φ, where Φ^T denotes the matrix transpose or adjoint of Φ and the elements of this matrix are measured in ml/virion/h. In the case of *E.coli*-T3 interactions we assume a modified gene-for-gene infection matrix (equation (1) of the main text; Forde et al 2008) but we also consider the following alternative infection mechanisms where σ represents the attachment rate of the wild type phage.

The form of the matching alleles Φ_{MA} and the gene-for-gene Φ_{GFG} infection matrix is defined in Agrawal and Lively (2002) as:

$$\Phi_{MA} = \sigma \begin{pmatrix} 1 & 0 & 0 & 0 \\ 0 & 1 & 0 & 0 \\ 0 & 0 & 1 & 0 \\ 0 & 0 & 0 & 1 \end{pmatrix}$$

and

$$\Phi_{GFG} = \sigma \begin{pmatrix} 1 & (1-p) & (1-p) & (1-p)^2 \\ 0 & (1-p) & 0 & (1-p)^2 \\ 0 & 0 & (1-p) & (1-p)^2 \\ 0 & 0 & 0 & (1-p)^2 \end{pmatrix},$$

where the parameter *p* represents a cost for a phage virulence allele. This form assumes that resistant host is always completely resistant. Throughout the paper we set p=0.4 and we note that changing the costs gave qualitatively similar results.

Given the above Φ_{MA} and Φ_{GFG}, we define the inverse matching alleles (Φ_{IMA}) and the inverse gene-for-gene (Φ_{IGFG}) infection matrices as:

$$\Phi_{IMA} = \sigma \begin{pmatrix} 0 & 1 & 1 & 1 \\ 1 & 0 & 1 & 1 \\ 1 & 1 & 0 & 1 \\ 1 & 1 & 1 & 0 \end{pmatrix},$$

and

$$\Phi_{IGFG} = \sigma \begin{pmatrix} 0 & 0 & 0 & (1-p)^2 \\ 0 & 0 & 0 & 0 \\ 0 & 0 & 0 & 0 \\ 0 & 0 & 0 & 0 \end{pmatrix}.$$

In addition we also consider the gene-for-gene and the inverse gene-for-gene infection matrices defined in (Fenton et al. 2009) where there is no cost for a phage virulence allele (p=0) but host can be partially resistant to phage ($\lambda<1$). In that case

$$\Phi_{GFG} = \sigma \begin{pmatrix} 1 & 1 & 1 & 1 \\ \lambda & 1 & \lambda & 1 \\ \lambda & \lambda & 1 & 1 \\ \lambda^2 & \lambda & \lambda & 1 \end{pmatrix},$$

and

$$\Phi_{IGFG} = \sigma \begin{pmatrix} \lambda^2 & \lambda & \lambda & 1 \\ \lambda^2 & \lambda^2 & \lambda & \lambda \\ \lambda^2 & \lambda & \lambda^2 & \lambda \\ \lambda^2 & \lambda^2 & \lambda^2 & \lambda^2 \end{pmatrix},$$

where we set $\lambda=0.2$. We find that the results are qualitatively the same for the different definitions of gene-for-gene and inverse gene-for-gene infection mechanisms.

Mutations

We use the matrix M_b as the genetic model for mutations in *E.coli* based on the assumption that mutations conferring resistance to T3 occur on two statistically independent loci: the first, L controls the synthesis of sugars required for LPS assembly and the second, O controls the concentration of proteins produced by the bacterium that are needed for the assembly of outer membrane protein (OMP) porin trimers. We assumed that point mutations occur at either locus at rate ε so that

$$M_b = I + \varepsilon(M_1 - 2I) + \varepsilon^2(M_2 - I),$$

where I is a 4x4 identity matrix and the term ε^2 arises due to the possibility that two mutations can occur simultaneously at both loci. The matrices M_1 and M_2 are given by

$$M_1 = \begin{bmatrix} 0 & 1 & 1 & 0 \\ 1 & 0 & 0 & 1 \\ 1 & 0 & 0 & 1 \\ 0 & 1 & 1 & 0 \end{bmatrix} \text{ and } M_2 = \begin{bmatrix} 0 & 0 & 0 & 1 \\ 0 & 0 & 1 & 0 \\ 0 & 1 & 0 & 0 \\ 1 & 0 & 0 & 0 \end{bmatrix}.$$

We also assumed that mutations in wild type phage (P_0) occur at one locus with four possible alleles giving rise to one of three types, denoted P_i (where i is from 1 to 3). The rate of mutations from one phage type to another is represented by ε□ĩwhich may be different from the mutation rate of bacteria also called ε above) and is independent of the type of phage. The mutation matrix M_p is defined as

$$M_p = I + \varepsilon(M_q - I),$$

where

$$M_q = \begin{bmatrix} 0 & 1 & 1 & 1 \\ 1 & 0 & 1 & 1 \\ 1 & 1 & 0 & 1 \\ 1 & 1 & 1 & 0 \end{bmatrix}.$$

The model

In a specific resource environment, the model used to study bacteria-phage coevolutionary dynamics is given by:

$$\begin{aligned} \frac{dS}{dt} &= D(S_0 - S) - c\mu(S)(B)^T \\ \frac{dB}{dt} &= M_b(\mu(S) \times B) - (\Phi P) \times B - DB \\ \frac{dP}{dt} &= M_P(\beta \times (\Phi^T B) \times P) - DP \end{aligned} \qquad (1)$$

where μ(S) denotes the vector of growth rates ($\mu_0(S)$, $\mu_1(S)$, $\mu_2(S)$, $\mu_3(S)$), S_0 is the concentration of glucose in a supply vessel that supplies the abiotic resource to the chemostat at rate D and c is a resource conversion factor that we assume to be a scalar constant. In addition $\beta = (\beta_0, \beta_1, \beta_3, \beta_4)$ represents a vector of burst rates with $\beta_0 > \beta_1 > \beta_3 > \beta_4$.

In the main text we extend the above model (1) to study bacteria-phage coevolutionary dynamics across different resource gradients and in the presence of gene flow between different resource environments.

Appendix B:

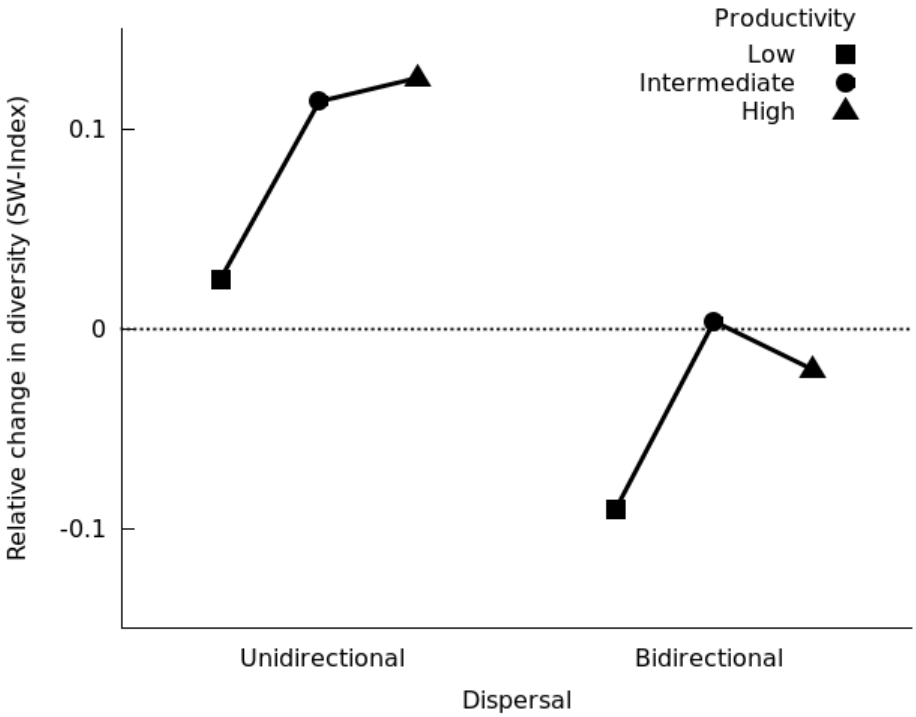

Figure B1: Relative changes in bacterial diversity for unidirectional and bidirectional dispersal treatment compared to no dispersal, predicted by model (2) of the main text with gene-for-gene infection mechanism.

(a)

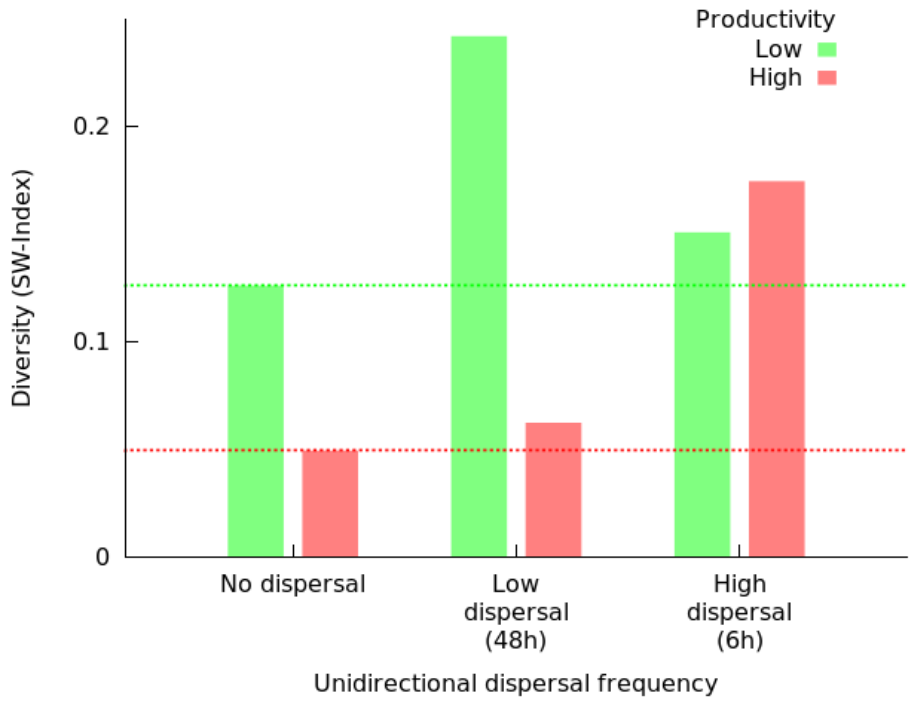

(b)

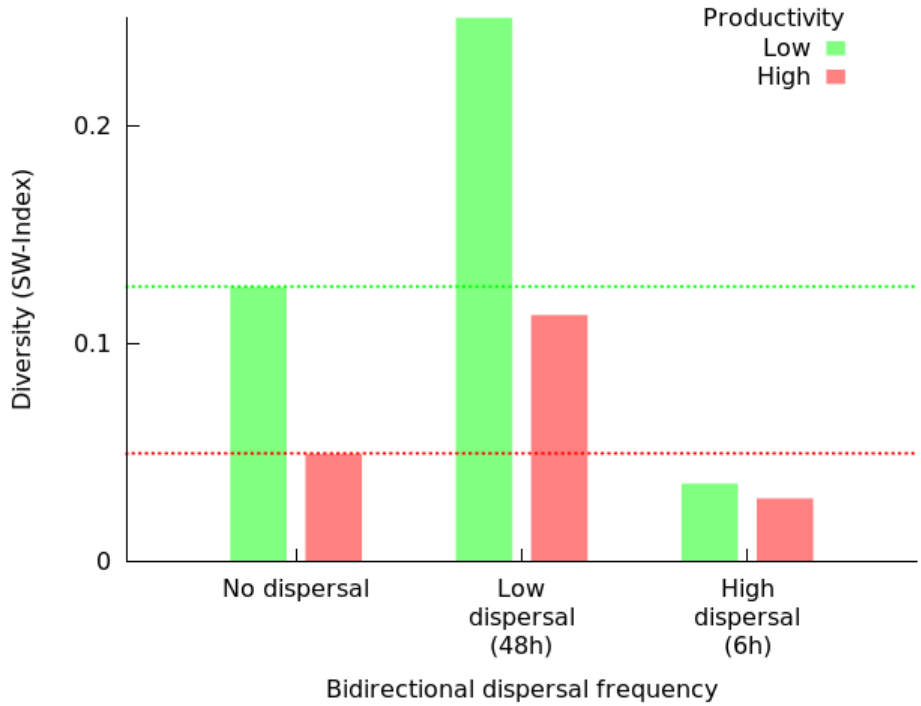

Figure B2: Bacterial diversity as a function of dispersal frequency, as predicted by model (2) with (a) unidirectional and (b) bidirectional dispersal.

References:

Agrawal, A. & Lively, C. M. (2002). Infection genetics: gene-for-gene versus matching alleles models and all points in between. *Evolutionary Ecology Research* **4**: 79–90.

Fenton, A., Antonovics, J. & Brockhurst M.A. 2009. Inverse-gene-for-gene infection genetics and coevolutionary dynamics. *Am. Nat.* **174**:230-242.

Ferris, M. T., Joyce. P. & Burch C. L. 2007. High Frequency of Mutations that Expand the Host Range of an RNA Virus. *Genetics* **176**: 1013-1022.

Forde, S., Beardmore, R., Gudelj, I., Arkin, S., Thompson, J., & Hurst, L. 2008. Understanding the limits to generalizability of experimental evolutionary models. Nature **455**: 220-224.

Gamow, R. I. 1969. Thermodynamics Treatment of Bacteriophage T4B Adsorption Kinetics. *Journal of Virology* **4**: 113-115